



This is a repository copy of *Reduced mechanism generation for methanol-based toluene reference fuel with combined reduction methods*.

White Rose Research Online URL for this paper:  
<http://eprints.whiterose.ac.uk/144646/>

Version: Accepted Version

---

**Article:**

Zhang, J. and Zhang, Y. [orcid.org/0000-0002-9736-5043](https://orcid.org/0000-0002-9736-5043) (2019) Reduced mechanism generation for methanol-based toluene reference fuel with combined reduction methods. *Fuel*, 247. pp. 135-147. ISSN 0016-2361

<https://doi.org/10.1016/j.fuel.2019.03.028>

---

Article available under the terms of the CC-BY-NC-ND licence  
(<https://creativecommons.org/licenses/by-nc-nd/4.0/>).

**Reuse**

This article is distributed under the terms of the Creative Commons Attribution-NonCommercial-NoDerivs (CC BY-NC-ND) licence. This licence only allows you to download this work and share it with others as long as you credit the authors, but you can't change the article in any way or use it commercially. More information and the full terms of the licence here: <https://creativecommons.org/licenses/>

**Takedown**

If you consider content in White Rose Research Online to be in breach of UK law, please notify us by emailing [eprints@whiterose.ac.uk](mailto:eprints@whiterose.ac.uk) including the URL of the record and the reason for the withdrawal request.



[eprints@whiterose.ac.uk](mailto:eprints@whiterose.ac.uk)  
<https://eprints.whiterose.ac.uk/>

# Reduced mechanism generation for methanol-based toluene reference fuel with combined reduction methods

Jing Zhang\*, Yang Zhang

(Department of Mechanical Engineering, The University of Sheffield, Sir Frederick Mappin Building, Sheffield S1 3JD, United Kingdom)

(E-mail: [JZhang155@sheffield.ac.uk](mailto:JZhang155@sheffield.ac.uk) (J. Zhang), [yz100@sheffield.ac.uk](mailto:yz100@sheffield.ac.uk) (Y. Zhang))

**Abstract:** TRF is a very competitive substitute fuel of gasoline, and methanol as a high octane oxygenated fuel has been attracted widely attention. In this study, a new reduced mechanism for methanol-based toluene reference fuel was developed based on the sensitivity analysis (SA), and reaction pathways analysis methods. At first, reduced mechanisms of methanol (including 24 species and 57 elementary reaction) and TRF (including 98 species and 264 elementary reaction) were developed and validated separately. Then, coupling methanol and TRF reduced mechanisms that have been validated in above section, a new reduced mechanism for methanol blending with TRF fuel was proposed that including 100 species and 290 elementary reactions. Extensive validations were performed by comparing experimental data of shock tube ignition delay times, flow reactor species profiles, pressure profiles with simulation results. High accuracy is demonstrated in wide ranges of temperature ( $T=300\sim 2500\text{K}$ ) and equivalence ratio ( $\Phi=0.375\sim 2$ ), which indicates that the present methanol blending with TRF fuel reduced mechanism can well predict the experimental data.

**Key words:** Methanol; Toluene reference fuel; Mechanism Reduction; Sensitivity analysis; Reaction pathways analysis method

## 1 Introduction

Increasingly severe fossil energy shortage and environmental problems promote many new combustion technologies used in internal combustion engines. In recent years, for example, homogeneous charge compression ignition (HCCI), low temperature combustion (LTC) with its high efficiency and low emission have won the favor of the majority of researchers. The LTC technology [1] controls the combustion temperature by combining modes of pre-mixing and compression-ignition, which means that fuel mixed with air form a uniform premixed gas before the compression process happened. As temperature rises, multiple points are simultaneously ignited in the cylinder. Therefore, it contributes to reduce NO<sub>x</sub> and hydrocarbon emissions and maintain high thermal efficiency, because of lower in-cylinder temperature. Lots of studies found that both of the HCCI and LTC combustion are ignited by the compression from the piston motion [2,3,4,5], so the chemical kinetics play key role in these processes [6,7]. Therefore, understanding the

32 reaction kinetics of hydrocarbon fuels can provide an important theoretical guidance for the development of  
33 internal combustion engines.

34 In addition to adopting new combustion theories, biofuels, like alcohol and biodiesel, are regarded as  
35 promising substitute fuels to be used in engines. Methanol has high octane value and oxygen content, which  
36 can improve fuel economy and reduce exhaust pollutants [8]. Another advantage is that methanol can be  
37 synthesized from fossil fuels and can also be extracted from biomass [9]. Therefore, it is considered as an  
38 additive fuel in this study.

39 Gasoline fuel is a mixture of hundreds or thousands of components including linear alkanes, branched  
40 alkanes, cycloalkanes, alkenes, aromatic hydrocarbons, etc. It is widely believed that the physicochemical  
41 properties of gasoline fuel can be characterized by part of major components [10]. At first, iso-octane was  
42 often used as an alternative fuel because of its similar physical and chemical properties with the gasoline.  
43 Later, considering the effect of octane number, mixture of n-heptane and isooctane (the primary reference  
44 fuel (PRF)) was used to characterize the gasoline octane number[11]. Generally, the gasoline contains 20%-  
45 50% of aromatic hydrocarbons, of which toluene is a representative component of aromatic hydrocarbons  
46 [12]. As a result, toluene gradually becomes one of main components for characterizing gasoline fuel. A  
47 mixture of n-heptane, isooctane and toluene in different proportions, also known as toluene reference fuel  
48 (TRF), has been used to represent gasoline. Table 1 shows several specific parameters for the three  
49 components in TRF[13], which clearly demonstrates its basic physicochemical properties.

50

Table 1. Specific parameters for the three components in TRF

Parameter name	iso-octane	n-heptane	toluene
Molecular formula	$(\text{CH}_3)_2\text{CHCH}_2\text{C}(\text{CH}_3)_3$	$\text{CH}_3(\text{CH}_2)_5\text{CH}_3$	$\text{C}_6\text{H}_5\text{CH}_3$
Molecular weight	114.23	100.20	92.14
C/H ratio	4:9	7:16	7:8
Density(20°C)/(g/ml)	0.6910~0.6930	0.682~0.685	0.865~0.869
Boiling point /°C	99.25	98.50	110.80
Low heating value /(MJ/kg)	44.65	44.93	40.94

51 Actually, the methanol detailed mechanism has been developed for many years. Bowman[14] first  
52 proposed a detailed chemical kinetic mechanism for methanol oxidation, but the model is inaccurate to  
53 predict experimental results when the temperature is below 1800 K[15]. Subsequently, Aronowitz et al.[16]  
54 constructed a kinetics model for methanol oxidation over the intermediate temperature range by experimental  
55 study using an adiabatic flow reactor under atmospheric conditions. In the same year, Westbrook and Dryer  
56 et al.[17] used shock tube and flow reactor to measure the reaction rates of some dominant species, and  
57 constructed a kinetic model of methanol oxidation that is adoptable over a wide range of conditions. The one-

58 dimensional flame propagation rate of this model under stoichiometric ratio condition can be well predicted.  
 59 Thomas et al.[18] corrected the methanol mechanism proposed by Tsang et al.[19]. The modified mechanism  
 60 greatly improved the simulation accuracy on the flow reactor. Flow analysis provides a further understanding  
 61 of the important reactions in the methanol oxidation process. The detailed chemical kinetic mechanism of  
 62 methanol proposed by Held and Dryer et al.[15] has good agreement with experimental data at various  
 63 situations. Since then, Li et al. [20] have used some new thermodynamic data of GRI-Mech 3.0[21] to  
 64 improve the mechanism developed by Held and Dryer et al.[15]. It is found that prediction performance of  
 65 this mechanism under a wide range of experimental conditions is better than that of Held and Dryer et al.[78],  
 66 especially in the simulation of the ignition delay time. In 2011, detailed kinetic mechanism of methanol  
 67 constructed by Zhang et al.[22] by considering the effects of CH, CH<sub>2</sub>(S) and CH<sub>2</sub>(T) radicals and nitrogen-  
 68 oxides. In this mechanism, the reaction rate constant of C/H/O is derived from the mechanism of Held and  
 69 Dryer et al.[15], and the stratification of CO/H<sub>2</sub>O/H<sub>2</sub>/O<sub>2</sub>, CH<sub>2</sub>O and CH<sub>3</sub>OH in Li et al.[20] were added. The  
 70 mechanism is verified by shock tubes and flow reactor experiments. In 2016, Burke et al.[23] first built a  
 71 new methanol chemical kinetic model (Mech 15.34), which accurately simulates methanol combustion  
 72 characteristics over a wide range of experimental conditions, especially when the pressure achieve at 10-50  
 73 atm. It has been extensively validated by experiments and previous studies. However, this mechanism has a  
 74 slight deviation from the experimental data of the stirred reactor when predicting the concentration of  
 75 formaldehyde. From above analysis, the methanol mechanism proposed by Zhang et al.[87] is adopted in  
 76 current study, due to its wide operating range. Some chemical kinetic mechanisms of methanol are  
 77 summarized in Table 2.

78 Table 2. Overview of methanol chemical kinetic mechanisms

Time	Literatures	Species	Reactions	T/K	p/atm	$\Phi$	Experiments
1975	Bowman et al. [14]	14	28	1545-2180	1.8-4.6	0.375-6.0	IDT(ST)
1979	Aronowitz et al. [16]	18	37	950-1030	1	0.03-3.16	SP(FR)
1979	Westbrook et al. [17]	26	84	1000-2180	1.0-5.0	0.05-3.0	IDT(ST), SP(FR)
1998	Held et al. [15]	22	89	633-2050	0.26-20.0	0.05-2.6	IDT(ST), SP(FR), LFV(SF)
2007	Li et al. [20]	18	84	300-2200	1.0-20.0	0.05-6.0	IDT(ST), SP(FR), LFV(SF)
2011	Zhang et al. [22]	46	247	800-2500	1.0-2.5	0.83-1.6	IDT(ST), SP(FR)
2016	Burke et al. [23]	173	1011	820-1650	2-50	0.5-2.0	IDT (ST,RPM), SP(JSR)

79 IDT: Ignition Delay Time; SP: Species Profile; LFV: Laminar Flame Velocity; ST: Shock Tube;  
 80 JSR: Jet Stirred Reactor; CF: Counter-flow Flame; SF: Spherical Flame; FR: Flow Reactor; RPM:  
 81 Rapid Compression Machine;

82 The toluene chemical kinetics mechanism has also attracted extensive attention, several typical chemical  
 83 kinetic models for TRF are presented in Table 3. Zhang et al.[24] added the toluene mechanism in PRF  
 84 mechanism and improved it to form a simplified TRF mechanism. Heghes et al.[25] modified the mechanism  
 85 of toluene based on a detailed PRF mechanism proposed by Andrae et al.[13]. Mehl et al.[26] of Lawrence  
 86 National Laboratory developed a detailed TRF chemical kinetic mechanism that is well matched to  
 87 experimental data over a wide range of pressures, temperatures, and equivalence ratios.

88 Table 3. Overview of TRF chemical kinetic mechanisms

Time	Literatures	Species	Reactions	T/K	p/atm	$\Phi$	Experiment s
2007	Andrae et al. <sup>[27]</sup>	1083	4635	800-1450	10-50	0.3-1	ST, HCCI
2009	Zhang et al. <sup>[24]</sup>	70	196	320-1800	1-42	0.5-2	ST, HCCI
2009	Heghes et al. <sup>[25]</sup>	1087	4639	700-1200	30-55	0.5-2	ST, HCCI
2009	Sakai et al. <sup>[28]</sup>	783	2883	500-1700	2-50	0.25-1	ST, FR
2011	Ra et al. <sup>[29]</sup>	113	487	870-1650	13-40	0.3-2	ST, HCCI

89 Further considering fuel chemical reaction mechanism gives an insight of pollutant emission and  
 90 thermodynamic analysis in engine operation process. Because of the complexity of the detailed mechanisms  
 91 and the significant stiffness induced by the highly reactive radicals, it is impractical to couple detailed  
 92 chemical kinetic mechanism with multidimensional CFD model directly, which could be far beyond the  
 93 current computing capability. So, there is a strong need to reduce chemical kinetic mechanisms which still  
 94 retain the essential dynamic features of the reaction system in a wide range of IC engine operating conditions.  
 95 In this paper, the reduced kinetic mechanism of methanol blending with toluene reference fuels is developed  
 96 by combining the methods of sensitivity analysis and reaction path analysis. Moreover, extensive validated  
 97 were performed by comparing experimental data of shock tube ignition delay times, flow reactor species  
 98 profiles, pressure profiles with simulation results.

## 99 2. Mechanism reduction method

### 100 2.1 Methodology for sensitivity analysis

101 The sensitivity analysis (SA) method is mainly to analyze the response of the system to small  
 102 disturbances, and the response value is sensitivity. The sensitivity coefficient can be obtained by solving a  
 103 set of partial differential equations, and then the importance of each reaction can be determined by comparing  
 104 the magnitude of each reaction sensitivity coefficient. Removing the less influential reactions is very  
 105 important to get a preliminary simplified reaction kinetic mechanism.

106 Considering the sensitivity of temperature to the rate constant of the elementary reactions is the  
107 temperature sensitivity coefficient, which can be written as[30]:

$$108 \quad S_T = \frac{k_j}{T} \frac{\partial T}{\partial k_j} = \frac{\partial \ln T}{\partial \ln k_j} \quad (1)$$

109 Where  $S_T$  is the orthogonal temperature sensitivity coefficient, and  $T$  is the system temperature, and  $k_j$   
110 is the parameter of the  $j$ th reaction in the mechanism.

111 The SA method can greatly simplify the reaction mechanism by effectively analyzing the dependence  
112 among the interrelated reactions and deleting the secondary reactions. However, it has shown that there are  
113 problems in the application process if only uses SA, as the reduced mechanism are unstable, and other  
114 methods are still needed to be adopted for improving its accuracy.

## 115 2.2 Methodology for reaction rate analysis

116 The reaction rate analysis method can analyze the effect of each elementary reaction on the net  
117 production rate of a specific specie. This method is widely used in chain reactions analysis, so that the  
118 reactions experienced the chain propagation process can be quickly obtained. In the calculation, the reaction  
119 rate  $P_K$  of the specie  $K$  and the influence coefficient of the different elementary reaction on the reaction rate  
120 of the reactant  $K$  are calculated by the following formulas (2) and (3), respectively[30]:

$$121 \quad P_K = \omega_K = \sum_{i=1}^I v_{ki} q_i \quad (2)$$

$$122 \quad C_{ki}^p = \frac{\max(v_{ki}, 0) q_i}{\sum_{i=1}^I \max(v_{ki}, 0) q_i} \quad (3)$$

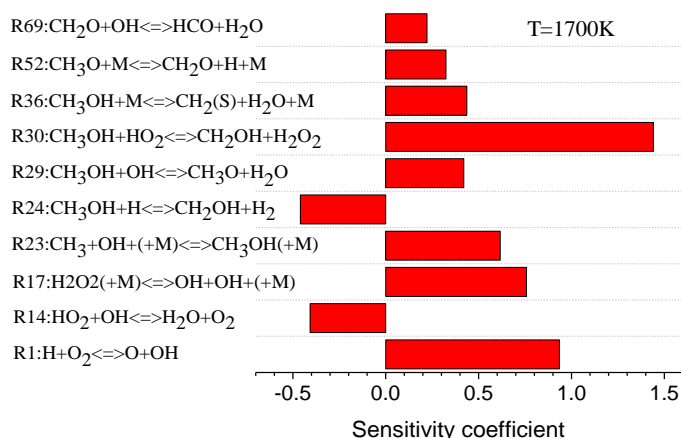
123 Where  $v_{ki}$  is the chemical equivalent coefficient of the  $i$ th elementary reaction, and  $q_i$  represents the  
124 reaction rate of the  $i$ th elementary reaction.  $I$  is the total number of all elementary reactions that contain  
125 reactant  $K$ . The importance of corresponding elementary reaction can be judged according to the ROP  
126 coefficient, which can be obtained by the Chemkin-Pro[31].

## 127 3. Develop and verify methanol and TRF blends reduced mechanism

### 128 3.1 Build reduced mechanism for methanol

129 First of all, it is significant to identify main intermediate species, as these species play a crucial role in  
130 chemical reaction process. The constant volume homogeneous batch reactor module in the Chemkin-Pro is  
131 used to calculate temperature sensitivity coefficients at the condition of  $\phi=1.0$ ,  $p=3.1$ atm and  $T=1700$ K. The  
132 sensitivity coefficient of the first ten reactions that have the greatest influence of temperature is listed in Fig.1  
133 by calculating the temperature sensitivity coefficient, as the sensitivity threshold is set to 0.001. If the  
134 sensitivity coefficient of a reaction is positive, it means that this reaction is more likely to promote combustion  
135 process, and vice versa.

136 Fig.1 indicates that the reaction R30:CH<sub>3</sub>OH + HO<sub>2</sub> = CH<sub>2</sub>OH + H<sub>2</sub>O<sub>2</sub> has the greatest influence on  
 137 CH<sub>3</sub>OH consumption process by H-atom abstraction. In addition, both of reaction R1:H + O<sub>2</sub> = O + OH and  
 138 R17:H<sub>2</sub>O<sub>2</sub> (+M) = OH + OH (+M) are sensitive to temperature. As rate of the reaction increases, a large  
 139 amount of heat is released when hydrogen peroxide is decomposed to hydroxyl, promoting the ignition  
 140 process and reducing the combustion ignition delay time. However, both of the reactions R14: HO<sub>2</sub> + OH =  
 141 H<sub>2</sub>O + O<sub>2</sub> and R24:CH<sub>3</sub>OH + H = CH<sub>2</sub>OH + H<sub>2</sub> are endothermic, so the temperature sensitivity coefficient is  
 142 negative. It is should be noted that hydroxyl radical is converted into a stable H<sub>2</sub>O molecule via reaction  
 143 R69:CH<sub>2</sub>O+OH<=>HCO+H<sub>2</sub>O, but this reaction is exothermic releasing lots of heat to promote ignition.  
 144 Therefore, species appearing in the above top ten most sensitivity reactions are determined as main  
 145 components, including CH<sub>3</sub>OH, H, OH, HO<sub>2</sub>, O<sub>2</sub>, CH<sub>2</sub>OH, CH<sub>3</sub>O, CH<sub>2</sub>(S), and CH<sub>2</sub>O, H<sub>2</sub>O, HCO, H<sub>2</sub>O<sub>2</sub>.

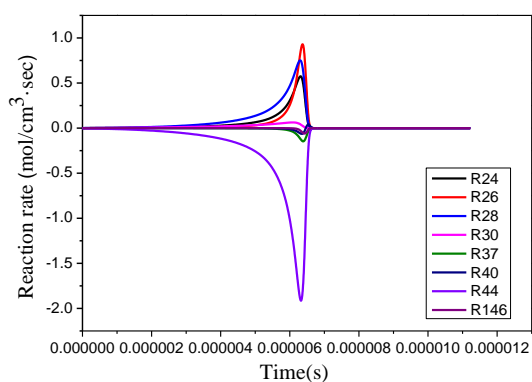
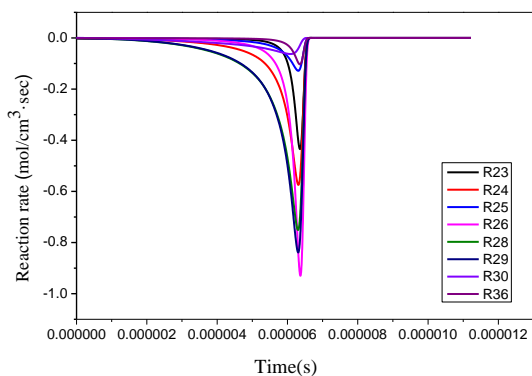


146

147 Fig.1. Temperature sensitivities at the time of ignition for methanol

148 In the next step, it is important to analyze key consumption pathways of these important intermediates  
 149 (CH<sub>3</sub>OH, CH<sub>2</sub>OH, CH<sub>3</sub>O, CH<sub>2</sub>(S), CH<sub>2</sub>O, HCO) by using the rate of reaction analysis method, thus those  
 150 paths that have opposite effects on the ignition delay time can be removed from detailed mechanism. It can  
 151 be seen from Fig.2, CH<sub>3</sub>OH is consumed by the reaction R26:CH<sub>3</sub>OH + O = CH<sub>2</sub>OH + OH, R28:CH<sub>3</sub>OH +  
 152 OH = CH<sub>2</sub>OH + H<sub>2</sub>O and R24:CH<sub>3</sub>OH + H = CH<sub>2</sub>OH + H<sub>2</sub>, so methanol mainly generated CH<sub>2</sub>OH with  
 153 small species such as with oxygen atom and hydroxyl radical by H abstraction reaction. However, CH<sub>2</sub>OH is  
 154 further oxidized generating an important intermediate product (CH<sub>2</sub>O) by the reaction R44:CH<sub>2</sub>OH + O<sub>2</sub> =  
 155 CH<sub>2</sub>O + HO<sub>2</sub>. In addition to formaldehyde mainly formed by reaction R44, the reaction R52:CH<sub>3</sub>O + M =  
 156 CH<sub>2</sub>O + H + M is also one of important production pathway. Reactions R67:CH<sub>2</sub>O + H = HCO + H<sub>2</sub> and  
 157 R71:CH<sub>2</sub>O + O<sub>2</sub> = HCO + HO<sub>2</sub> are the main consumption pathways of formaldehyde, so CH<sub>2</sub>O can be further  
 158 dehydrogenated to form aldehyde group (HCO). As shown in Fig.2 (d), CH<sub>2</sub>O is produced by the reaction  
 159 R29:CH<sub>3</sub>OH + OH = CH<sub>3</sub>O + H<sub>2</sub>O, and then consumed by the reaction R52 and R57:CH<sub>3</sub>O + O<sub>2</sub> = CH<sub>2</sub>O +  
 160 HO<sub>2</sub>. CH<sub>2</sub>(S) is mainly formed by the reaction R99:CH<sub>3</sub> + OH = CH<sub>2</sub>(S) + H<sub>2</sub>O and R36:CH<sub>3</sub>OH + M =  
 161 CH<sub>2</sub>(S) + H<sub>2</sub>O + M, and then consumed via R124:CH<sub>2</sub>(S) + M = CH<sub>2</sub>(T) + M, R118:CH<sub>2</sub>(S) + H = CH + H<sub>2</sub>

162 and R121:  $\text{CH}_2(\text{S}) + \text{OH} = \text{CH}_2\text{O} + \text{H}$ . It indicates that a small portion of methanol will occur decomposition  
 163 producing  $\text{CH}_2(\text{S})$  that can form formaldehyde by oxidation reaction. Finally, the H atom is abstracted in the  
 164 HCO group to form CO, and then CO is oxidized to  $\text{CO}_2$ .

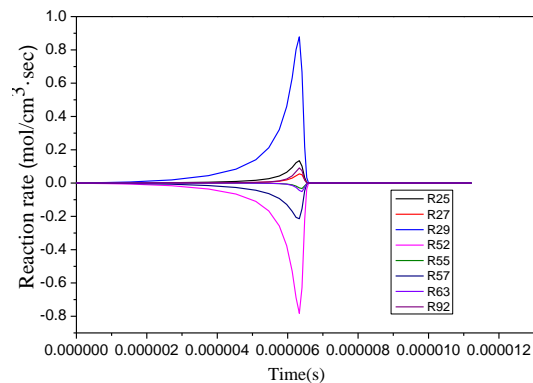
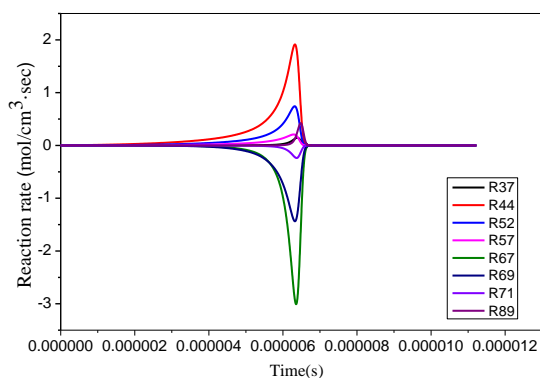


165

(a)  $\text{CH}_3\text{OH}$

(b)  $\text{CH}_2\text{OH}$

166

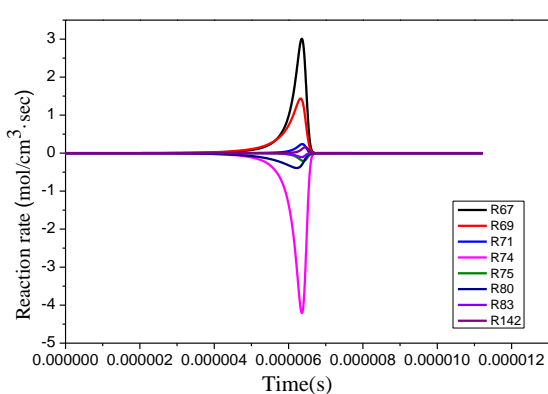
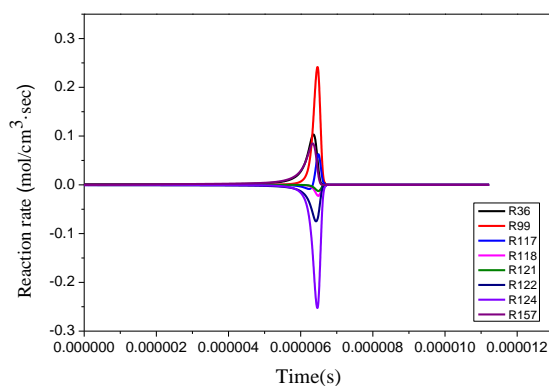


167

(c)  $\text{CH}_2\text{O}$

(d)  $\text{CH}_3\text{O}$

168

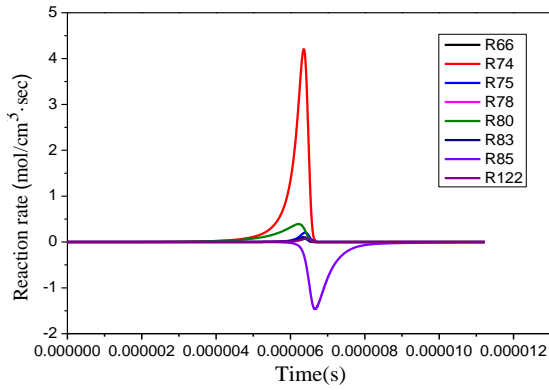


169

(e)  $\text{CH}_2(\text{S})$

(f) HCO

170



171

172

(g) CO

173

Fig.2. Reaction rate of some major intermediates in methanol reduced mechanism.

174

175

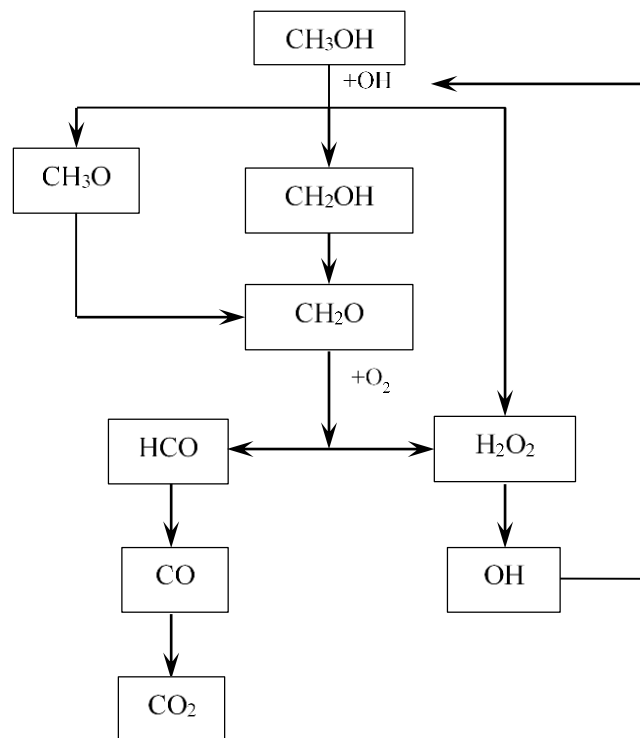
Combining the methods of SA and reaction rate analysis, the above processes were repeated, and reactions that reaction rate is above  $1e-6$  mole/cm<sup>3</sup>-sec are supposed to be remain in reduced mechanism.

176

Therefore, a reduced methanol mechanism including 24 species and 57 reactions was obtained, and its primary

177

oxidation pathways are shown in Fig.3.



178

179

Fig.3. Methanol primary oxidation pathways.

180

### 3.2 Validate methanol reduced mechanism

181

The ignition delay time is defined as the time, at which the products CO and O reach a maximum

182

concentration. Table 4 gives the simulation conditions for CH<sub>3</sub>OH/O<sub>2</sub>/Ar mixture according to the shock tube

183

experiments of Bowman et al.[14]. It can be seen from Fig.4 that the ignition delay time of methanol is

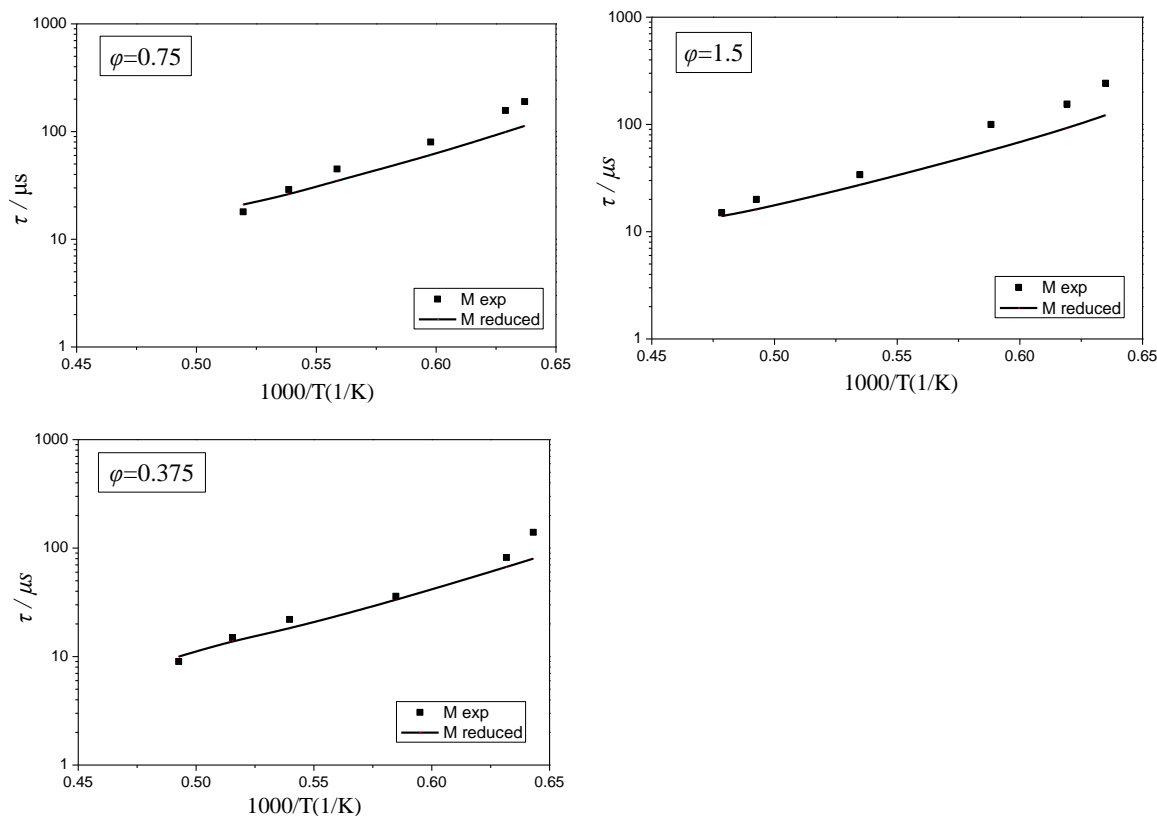
184

advanced with the increase of initial temperature. When the equivalence ratio is 0.375 and 0.75, predictions

185 that simulated via Chemkin-Pro are in good agreement with experimental data. Nevertheless, when the  
 186 equivalent ratio is 1.5, predicted value of the reduced mechanism is slightly lower than experimental data  
 187 because part of the species and reactions are removed, causing the pre-exponential factor and the activation  
 188 energy changed. However, the constructed reduced mechanism reflects that the ignition delay time decreases  
 189 with increasing temperature. It well captures ignition characteristics within the error tolerance during  
 190 methanol combustion process.

191 Table 4. CH<sub>3</sub>OH/O<sub>2</sub>/Ar mixture shock tube experiments parameters

Mixture	$\phi$	CH <sub>3</sub> OH/%	O <sub>2</sub> /%	Ar/%	Pressure/atm
1	0.75	2.00	4.00	94.00	1.40
2	1.5	1.00	1.00	98.00	3.10
3	0.375	1.00	4.00	95.00	2.95



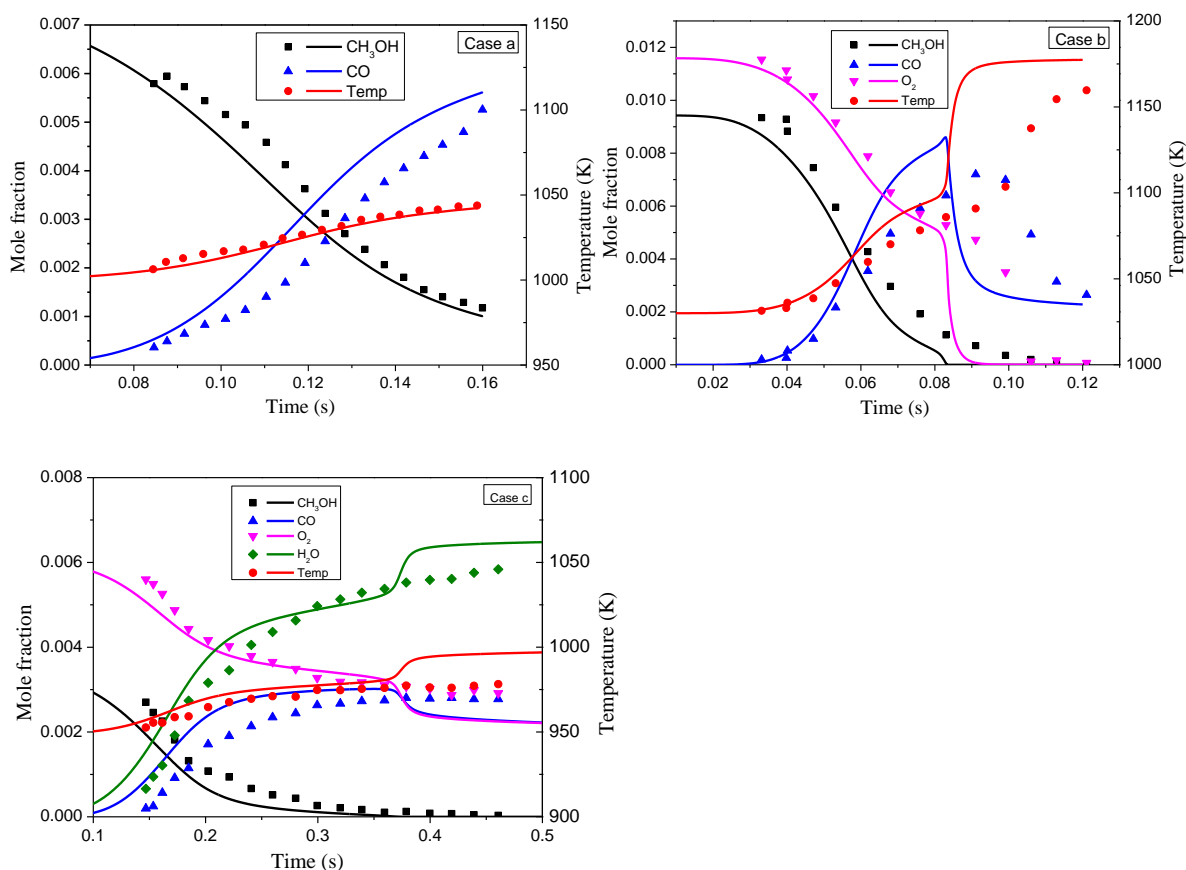
192  
 193  
 194 Fig.4. Comparison of the predicted ignition delay times between the methanol reduced mechanism and  
 195 experiments data at various equivalence ratio[14].

196 The flow reactor experiment essentially compensates for the gap between the static reactor and the shock  
 197 tube experiment for good understanding and developing the combustion dynamics. The flow reactor  
 198 experiment provides information at the low and medium temperature ranges, typically in the 800-1200K  
 199 temperature. The flow reactor is set to a homogeneous condition and is adiabatic. Aronowitz et al.[16], Norton  
 200 et al.[32] and Held et al.[15] simulated methanol oxidation in a flow reactor. Table 5 summarizes the

201 experimental conditions for the flow reactor. Fig.5 shows important species concentration file and  
 202 temperature file that calculated by the methanol reduced mechanism. For all cases, prediction of the CH<sub>3</sub>OH  
 203 and CO concentration are generally consistent with experimental measurements. As a result, the model is  
 204 able to well predict major species, while the temperature is a little bit over predicted at the end of combustion,  
 205 which mainly because the model that we assumed is adiabatic.

206 Table 5. The summation of the experimental conditions for the flow reactor

Case	Experiments	T/K	p/atm	$\phi$	CH <sub>3</sub> OH/%	O <sub>2</sub> /%	N <sub>2</sub> /%
a	Aronowitz et al. [16]	1000	1	1.6	0.735	0.6891	98.5759
b	Norton et al. [32]	1030	1	1.22	0.943	1.1594	97.8976
c	Held et al. [15]	949	2.5	0.83	0.333	0.6018	99.0652



207  
 208  
 209 Fig.5. Comparison of modeling and experimental results for major species concentration of methanol  
 210 (Signal represents experiments data, and line represents methanol reduced model predictions).

### 211 3.3 Build reduced mechanism for TRF

212 Based on the semi-detailed mechanism of TRF created by Andrae et al.[13], same methods are used to  
 213 reduce it like methanol mechanism reduced process. But there is difference between the simplified process  
 214 of methanol and TRF mechanism, because sensitivity analysis is no longer used to determine important

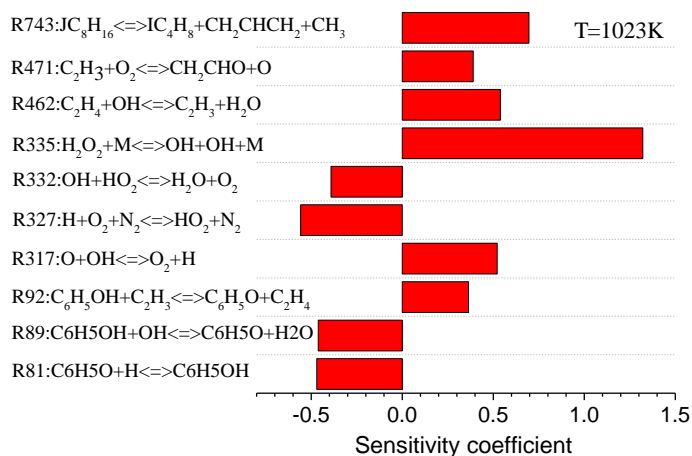
215 components in reaction process. The reactions that sensitivity coefficient greater than thresholds are  
 216 screened out directly, since the mechanism of TRF has many components and is more complicated than that  
 217 of methanol. Then the reaction rate analysis is used to find out its overall reaction pathway to develop a new  
 218 TRF reduced mechanism.

219 According to the experiments of Andrae[13], there are 7 different blends ratio of TRF, and it can be seen  
 220 in Table 6. In the case 6 and 7, fuels are blended according to liquid volume ratio, and others are mole volume  
 221 ratio. Giving different sensitivity thresholds can generate simplified mechanisms with different scales. The  
 222 higher the threshold is, the more species will be deleted, thereby giving rise to greater error. However,  
 223 fluctuation also occurs during the reduction process that can be seen when equivalence ratio is 0.5, because  
 224 the coupling strength among the species is different in mechanism, and the number of reactions and  
 225 components are discontinuous functions with the threshold changing. Four reduced TRF mechanisms and its  
 226 maximum errors are listed in Table 6, and each of them for 7 cases is validated by simulating ignition delay  
 227 time in shock tube model.

228 Table 6. Four reduced TRF skeleton mechanisms at various thresholds

Threshold	Species	Reactions	Maximum error/%
0.001	125	452	33.6
0.01	107	324	33.8
0.05	98	247	24.9
0.1	91	196	30.4

229 Considering accuracy and degree of simplify, the reduced mechanism that has 98 species and 247  
 230 reactions was regarded as the sub-mechanism of TRF. The most sensitivity coefficients of the top 10 reactions  
 231 is shown in Fig.6, at which the threshold is set as 0.05,  $T=1023K$ ,  $p=3.04Mpa$  and  $\phi=1$ .



232 Fig.6. Temperature sensitivity analysis at the time of ignition for TRF  
 233

234 It can be seen from Fig.6 that reaction R335: $H_2O_2 + M = OH + OH + M$  has greatest impact on  
 235 combustion temperature, since  $H_2O_2$  decomposes producing lots of OH radicals that will rapidly react with  
 236 other free radicals. Therefore, this reaction promotes system temperature rapidly. In addition, R743: $JC_8H_{16} =$   
 237  $IC_4H_8 + CH_2CHCH_2 + CH_3$  and R462: $C_2H_4 + OH = C_2H_3 + H_2O$  also have high temperature sensitivity. On  
 238 the other hand, R327: $H + O_2 + N_2 = HO_2 + N_2$  and R81: $C_6H_5O + H = C_6H_5OH$  are endothermic reactions, so  
 239 increasing their reaction rate can decrease the system temperature. Reaction R332:  $OH + HO_2 = H_2O + O_2$   
 240 and R89: $C_6H_5OH + OH = C_6H_5O + H_2O$  compete with other species to consume  $HO_2$  and OH, suppressing  
 241 TRF consumption and making heat release slows down.

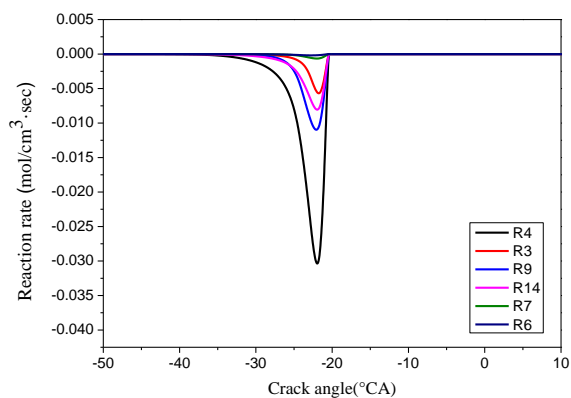
242 The TRF reduced mechanism includes the following parts: toluene mechanism, hydrocarbon small  
 243 molecule mechanism, n-heptane skeleton mechanism, isooctane skeleton mechanism. Part of reactions that  
 244 have been removed by the sensitivity analysis in the PRF are listed in Table 7, and are added in the final  
 245 reduced mechanism.

246 Table 7 Reactions that are supposed to be remain with its rate coefficients in Arrhenius form  $k=AT^n \exp(-$   
 247  $E/R^\circ T)$

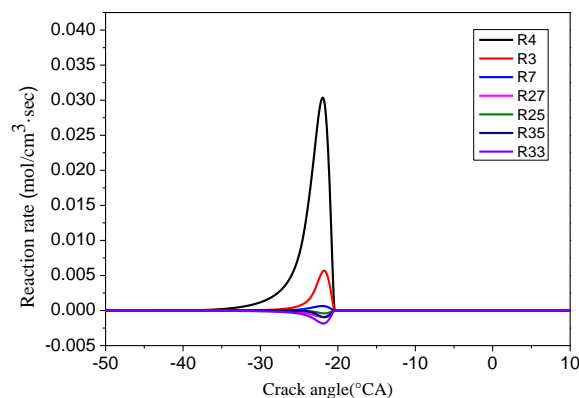
No.	Reactions	A	n	E
R705	$C_7H_{16} + O_2 \rightleftharpoons C_7H_{15} + HO_2$	6.000E+13	0.0	52820
R718	$C_7H_{14}O_2H + O_2 \rightleftharpoons O_2C_7H_{14}O_2H$	5.600E+12	0.0	0.0
R719	$O_2C_7H_{14}O_2H \rightleftharpoons HO_2C_7H_{13}O_2H$	2.000E+11	0.0	17010
R720	$HO_2C_7H_{13}O_2H \rightleftharpoons OC_7H_{13}O_2H + OH$	1.000E+09	0.0	7500
R722	$OC_7H_{13}O \rightleftharpoons CH_2O + C_5H_{11} + CO$	2.000E+13	0.0	15000
R725	$C_5H_{11} \rightleftharpoons C_2H_4 + I^*C_3H_7$	7.972E+17	-1.44	29876
R730	$I^*C_3H_7 + H \rightleftharpoons C_2H_5 + CH_3$	5.00E+13	0.0	0.0
R731	$PC_4H_9(+M) \rightleftharpoons C_2H_5 + C_2H_4(+M)$	1.06E+13	0.0	27828
R732	$PC_4H_9 \rightleftharpoons C_2H_5 + C_2H_4$	2.50E+13	0.0	28800
R734	$AC_8H_{17} + O_2 \rightleftharpoons AC_8H_{17}OO$	1.00E+12	0.0	0.0
R735	$AC_8H_{17}OO \rightleftharpoons AC_8H_{16}OOH-B$	1.14E+11	0.0	22400
R739	$OC_8H_{15}OOH \rightleftharpoons OC_8H_{15}O + OH$	3.98E+15	0.0	43000

248 Furthermore, toluene is different from n-heptane and iso-octane, due to its unique benzene ring structure.  
 249 The ring should be relieved in reaction process, and it is quiet complicated. The conventional reduced process  
 250 may neglect some toluene-specific reaction pathways. Therefore, the rate of production of some species  
 251 related to toluene is analyzed when  $T=500K$ ,  $p=2atm$ , and  $\phi=0.5$ . In Fig.7, toluene ( $C_6H_5CH_3$ ) is mainly  
 252 consumed by R4:  $C_6H_5CH_3 + OH = C_6H_5CH_2 + H_2$  and R9:  $C_6H_5CH_3 + O = OC_6H_4CH_3 + H$ , then  $C_6H_5CH_2$

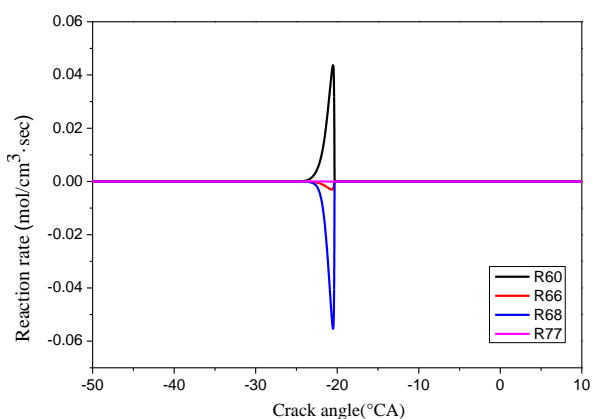
253 reacts with HO<sub>2</sub> and O<sub>2</sub> formed C<sub>6</sub>H<sub>5</sub>CHO and C<sub>6</sub>H<sub>5</sub>CH<sub>2</sub>OO via reactions R27: C<sub>6</sub>H<sub>5</sub>CH<sub>2</sub> + HO<sub>2</sub> = C<sub>6</sub>H<sub>5</sub>CH<sub>2</sub>O  
 254 + OH and R33: C<sub>6</sub>H<sub>5</sub>CH<sub>2</sub> + O<sub>2</sub> = C<sub>6</sub>H<sub>5</sub>CH<sub>2</sub>OO. The intermediate species benzene (C<sub>6</sub>H<sub>6</sub>) is mainly formed  
 255 by the decomposition of OC<sub>6</sub>H<sub>4</sub>CH<sub>3</sub> in the reaction R60: OC<sub>6</sub>H<sub>4</sub>CH<sub>3</sub> = C<sub>6</sub>H<sub>6</sub> + CO + H, and it is consumed  
 256 to phenyl (C<sub>6</sub>H<sub>5</sub>) and C<sub>6</sub>H<sub>5</sub>O by reaction R68: C<sub>6</sub>H<sub>6</sub> + OH = C<sub>6</sub>H<sub>5</sub> + H<sub>2</sub>O and R66: C<sub>6</sub>H<sub>6</sub> + O = C<sub>6</sub>H<sub>5</sub>O + H  
 257 respectively.



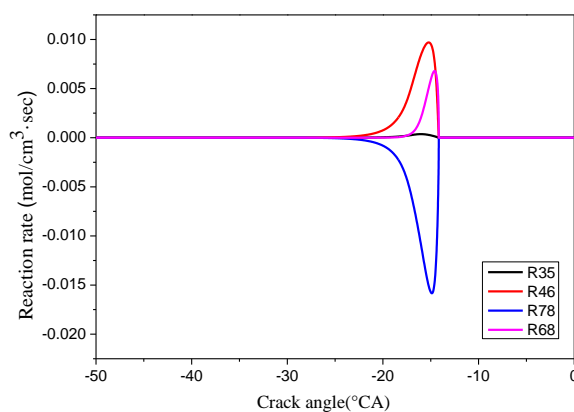
(a) C<sub>6</sub>H<sub>5</sub>CH<sub>3</sub>



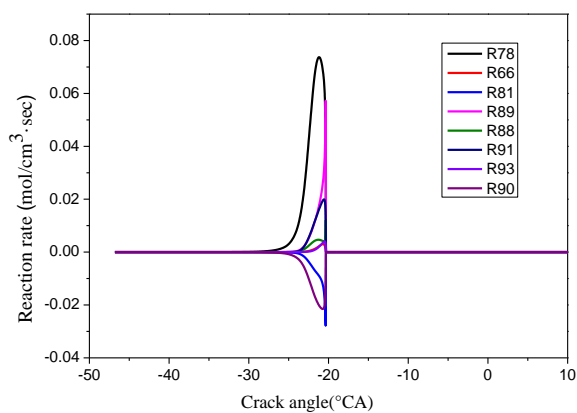
(b) C<sub>6</sub>H<sub>5</sub>CH<sub>2</sub>



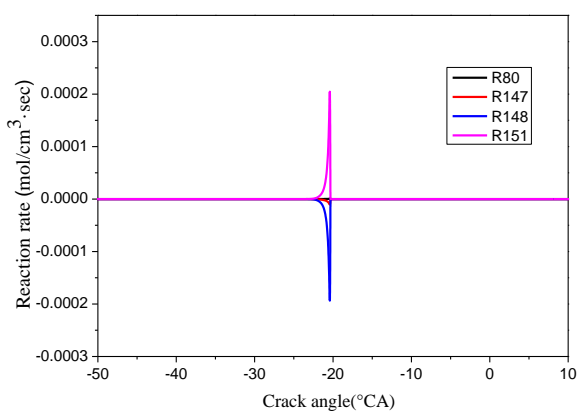
(c) C<sub>6</sub>H<sub>6</sub>



(d) C<sub>6</sub>H<sub>5</sub>



(e) C<sub>6</sub>H<sub>5</sub>O



(f) C<sub>5</sub>H<sub>5</sub>

Fig.7. Reaction rate of some major intermediates in TRF final reduced mechanism.

265 The TRF reduced mechanism, combining simplified toluene sub-mechanism, the PRF skeleton  
 266 mechanism and the hydrocarbon small molecule mechanism, can be obtained after sensitivity analysis and  
 267 reaction rate analysis, including 98 species and 264 elementary reactions.

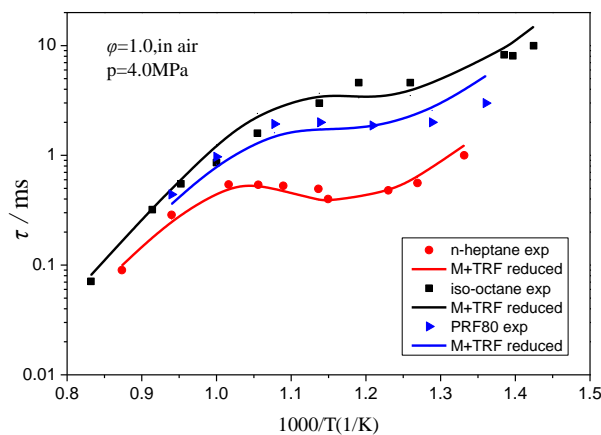
268 3.4 Validate TRF reduced mechanism

269 The ignition delay time verification for TRF under 7 different fuel blends cases[20] is performed, and it  
 270 can be seen in Table 8. In case 6 and 7, fuels are blended as liquid volume ratio, while others are mole volume  
 271 ratio. Fig.8-10 present the comparison of predicted ignition delay times and experimental data[33,34,35] in  
 272 shock tube accordingly.

273 Table 8. The initial conditions of shock tube experiments for TRF fuel.

Situation	$\phi$	C <sub>7</sub> H <sub>16</sub> /%	C <sub>8</sub> H <sub>18</sub> /%	C <sub>6</sub> H <sub>5</sub> CH <sub>3</sub> /%	p/Mpa
1	1.0	100	0	0	4.0
2	1.0	0	100	0	4.0
3	1.0	20	80	0	4.0
4	1.0	0	0	100	3.04
5	1.0	0	0	100	5.07
6	1.0	17	63	20	3.04
7	1.0	17	63	20	5.07

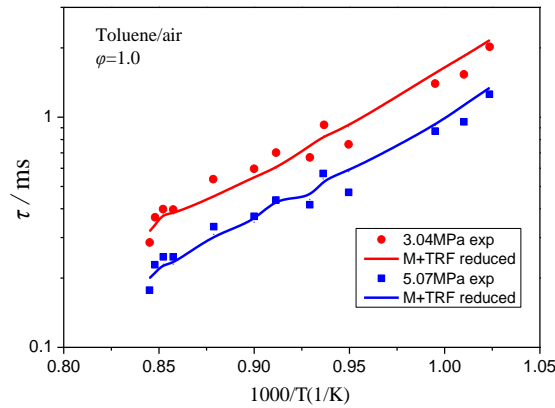
274 In Fig.8, the ignition delay times show clearly negative temperature coefficient (NTC) behavior for case  
 275 1, 2 and 3, and the predictions are well agreed with experimental value[33]. It can also explain the low  
 276 temperature response characteristics of TRF when temperature ranges from 850K to 1200K. As temperature  
 277 is above 1000 K, there is no significant difference of ignition delay time among these mixtures. Besides, it is  
 278 easy to see that the ignition delay time is advanced as octane number decreasing of a stoichiometric fuel/air  
 279 mixture. The n-heptane octane number is 0 and the iso-octane is 100. Overall, the dependence of ignition  
 280 delay time on octane is excellently consistent with the shock tube presentation.



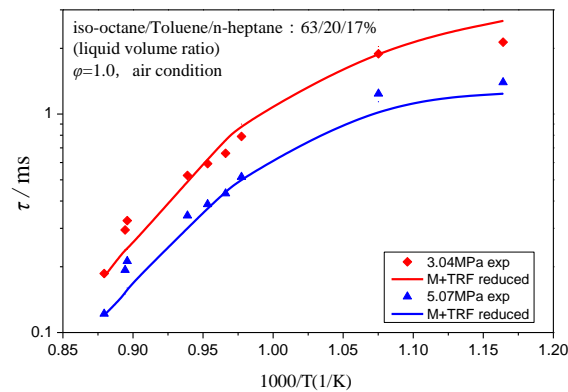
281

282 Fig.8. Ignition delay time of TRF for situation 1-3 (Signal represents experiments data[33], and line  
 283 represents predictions).

284 Fig.9 indicates that the TRF reduced mechanism can capture the tendency of ignition delay time with  
 285 temperature at 3.04 MPa and 5.07Mpa operating conditions[34]. It also can be found that the ignition delay  
 286 time predictions agree well with experimental data[35] in Fig.10. Besides, the ignition delay time decreases  
 287 with increasing pressure.



288  
 289 Fig.9. Ignition delay time of TRF for situation 4 and 5. (Signal represents experiments data[34], and  
 290 line represents predictions)



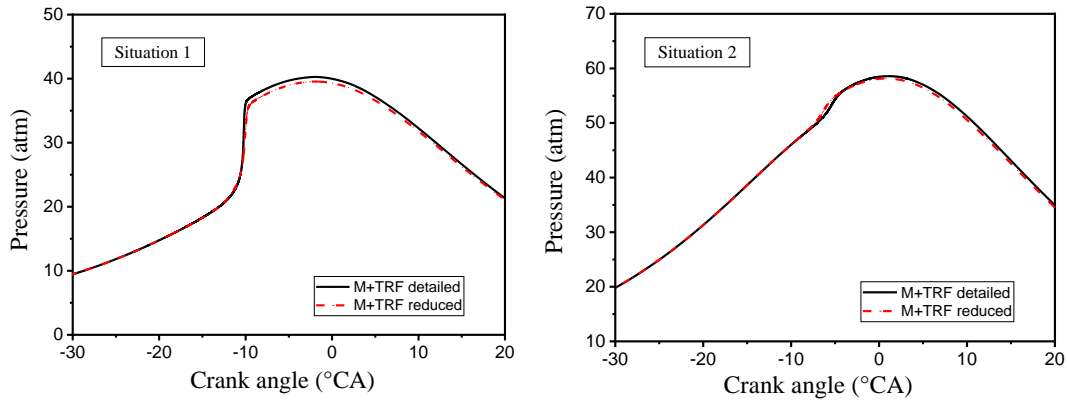
291  
 292 Fig.10 Ignition delay time of TRF for situation 6 and 7. (Signal represents experiments data[35], and  
 293 line represents predictions)

294 TRF is adopted in engines widely, so internal cylinder pressure can be used to vlify the accuracy of  
 295 TRF reduced mechanism in HCCI by using the zero-dimensional single-zone engine module in Chemkin-  
 296 Pro. Assuming that the combustion process is adiabatic, ignoring gas loss from the intake and exhaust.  
 297 Moreover, n-heptane / isooctane / toluene liquid volume ratio is 17/69/14, and engine speed is 1200rpm, and  
 298 compression ratio is 14.04, as shown in Table 9.

299 Table 9. Operating conditions in HCCI engine [36]

Situation	$\varphi$	$p/\text{Mpa}$	$T/\text{K}$	$n/\text{rpm}$
1	0.25	0.1	523	1200

300 Fig.11 shows the comparison of cylinder pressure between the simulation of TRF reduced and detailed  
301 mechanism at Andrae et al. experimental conditions [36]. In Fig.11, the predictions of peak pressure for both  
302 mechanisms show great agreement, presenting great prediction of ignition process in HCCI for TRF reduced  
303 mechanism.  
304

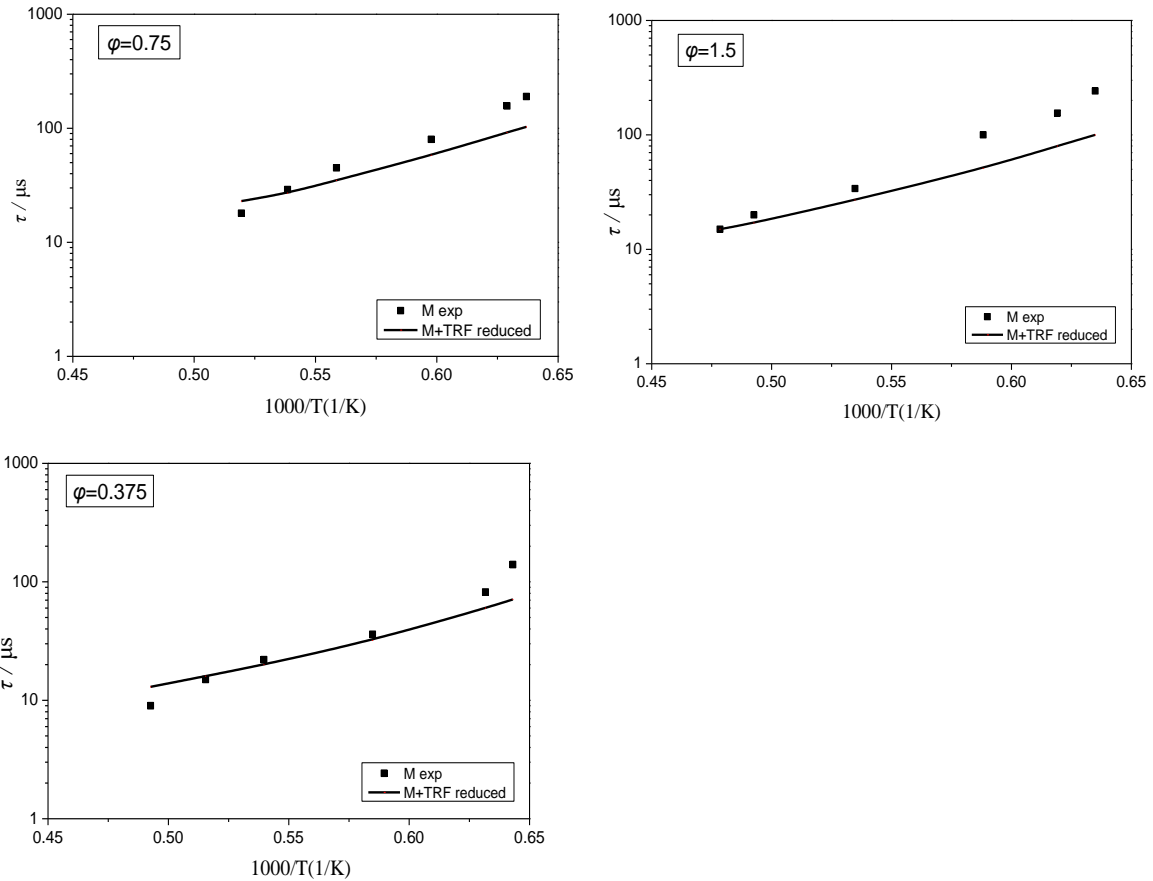


305  
306 Fig.11. Comparison of cylinder pressure between the simulation of TRF reduced mechanism and its  
307 detailed mechanism.

### 308 3.5 Validate methanol blending with TRF fuel reduced mechanism

309 Coupling methanol and TRF reduced mechanisms that have been validated in above section, a new  
310 reduced of mechanism for methanol blending with TRF fuel can be proposed that including 100 species and  
311 290 elementary reactions. After that extensive validation should be performed, so ignition delay time for  
312 methanol and TRF are supposed to be validated separately by comparing the simulation of the methanol and  
313 TRF blends reduced mechanism with experiments data, and the methanol shock tube experimental conditions  
314 can be found in Table 4.

315 It can be seen from the Fig.12 that the ignition delay time of methanol is advanced with the increase of  
316 temperature when equivalence ratio from 0.375 to 1.5. Although the prediction is slightly lower than  
317 experimental value [14], it still can be regarded that the constructed mixed reduced kinetic model can well  
318 predict methanol ignition delay time at the range of 1500-2100K.

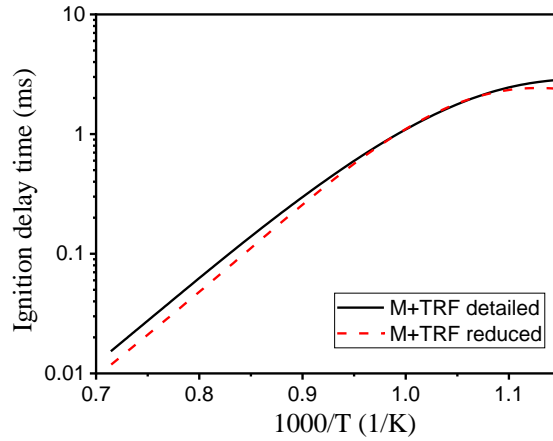


319

320

321 Fig.12. Comparison of the predicted ignition delay times between the mixed reduced mechanism and  
 322 experiments data at various equivalence ratio [14].

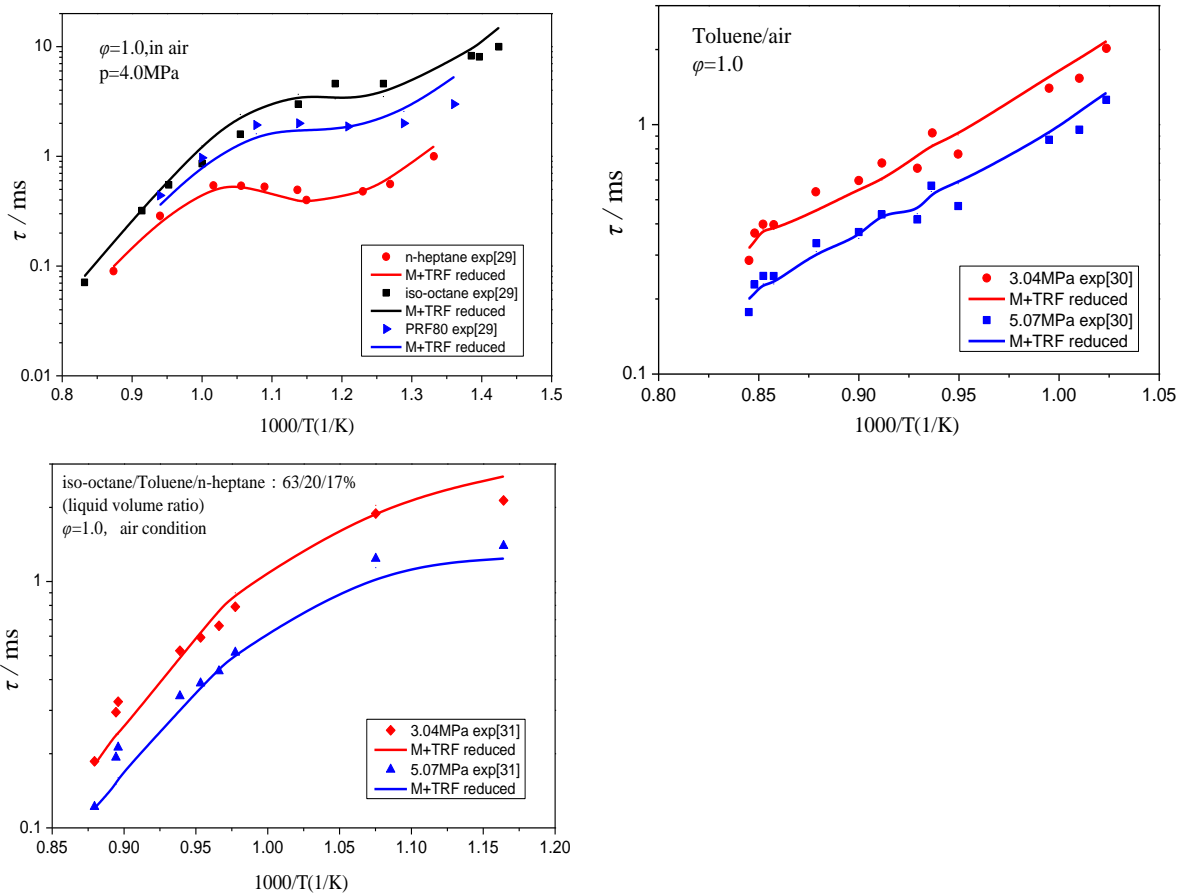
323 Initial simulation conditions of mixed reduced mechanism in shock tube can be found in Table 8. In  
 324 Figure 13, the comparison of M+TRF reduced mechanism and TRF detailed mechanism is presented at the  
 325 condition of 30atm and stoichiometric. A great agreement shows that reduced model can as good as detailed  
 326 mechanism predict ignition delay time at wide conditions. It can also be seen from the Fig.14 that ignition  
 327 delay times of the mixed reduced mechanism are in good agreement with experimental value [33,34,35].  
 328 Besides, the Fig.15 shows a comparison between the results of methanol-TRF reduced mechanism  
 329 calculations and the experimental results of the shock tube measurements for toluene by Davidson et al. [30].  
 330 Clearly, there is good agreement between the experimental data and the calculated data under the pressure of  
 331 3.04 MPa and 5.07 MPa, especially under relatively high temperature conditions. Overall, the mixed reduced  
 332 mechanism not only well captures the ignition characteristics at all pressure and temperature ranges, but also  
 333 can demonstrate the phenomenon that ignition delay time is advanced as the octane number decreases of a  
 334 stoichiometric fuel/air mixture.



335

336

Fig.13. Comparison of the predicted ignition delay times between the detailed and reduced mechanism.



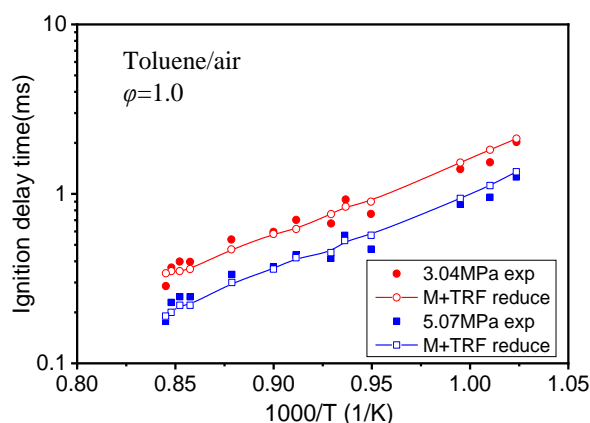
337

338

339

340

Fig.14. Comparison of the predicted ignition delay times of the mixed reduced mechanism at different experiments conditions[33-35].



341

342

Fig.15. Comparison of the predicted ignition delay times between the methanol-TRF reduced

343

mechanism and experiments data at different pressures[30].

344

Then, those important species in mixed reduced mechanism should be validated by comparing the

345

simulation of methanol and TRF blends reduced mechanism with experiments data[16,32,15]. Conditions for

346

the flow reactor simulation are shown in Table 5. Fig.16 shows that species concentration profile and

347

temperature profile of the mixed reduced mechanism are generally consistent with measurements in flow

348

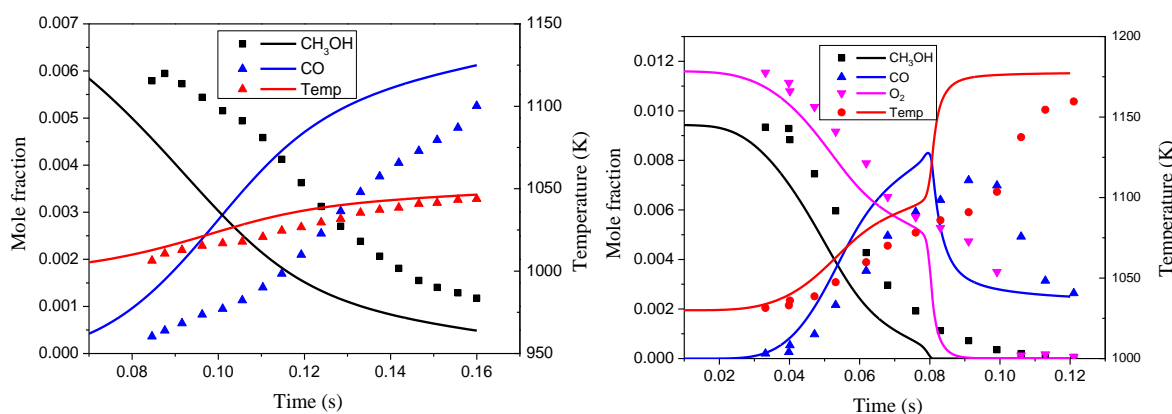
reactor. When equivalence ratio ranges from 0.375 to 1.5, the predicted peak value of  $\text{CH}_3\text{OH}$ ,  $\text{CO}$ ,  $\text{O}_2$  and

349

$\text{H}_2\text{O}$  are close to experimental data. Therefore, the methanol and TRF blends reduced chemical kinetic model

350

can be used to predict concentration variation of some important species in combustion process.



351

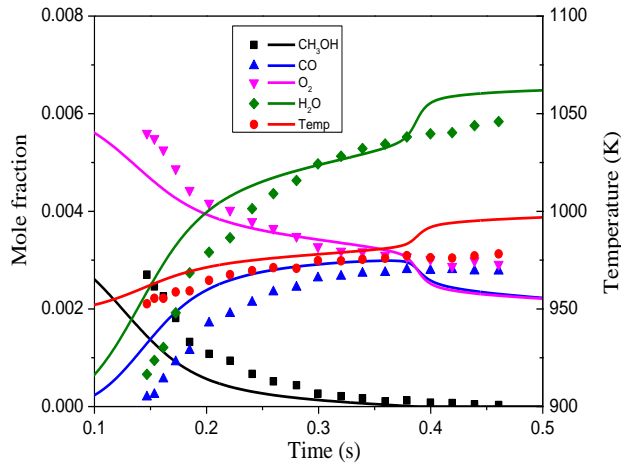


Fig.16. Comparison of modeling and experimental results for species concentration (Signal represents experiments data[16,32,15], and line represents methanol and TRF reduced model predictions).

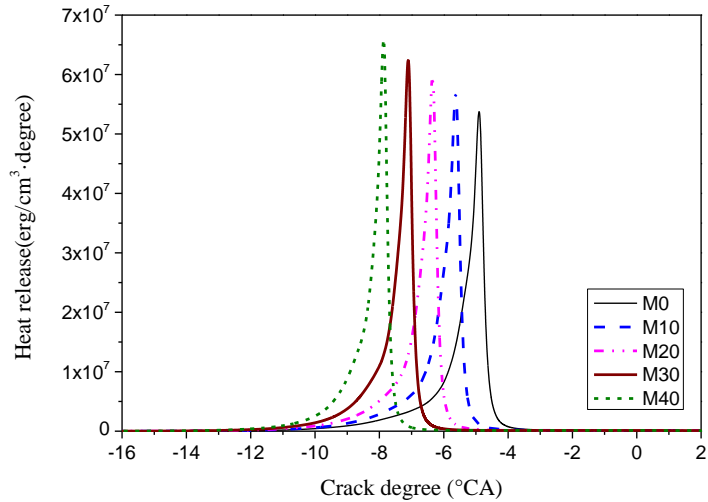
#### 4. The effect of methanol on TRF performance

In order to study the effect of methanol on TRF combustion and emission performance, we blend different ratio of methanol in TRF. The liquid volume ratio of the methanol in blends fuel is shown in Table 10.

Fig. 17 shows the heat release rate for different volume fractions of methanol in TRF fuel. The simulated HCCI engine conditions are shown in Table 9. Start timing of exothermic is advanced with the blending ratio of methanol fuel increasing, because methanol is a high-octane fuel and contains oxygen atom that can promote combustion complete. In addition, combustion duration decreases, while the peak of exothermic rate and total heat release increase gradually, since the addition of methanol inhibits the secondary oxidation reaction of other fuel components.

Table 10 The liquid volume ratio of methanol in blends fuel

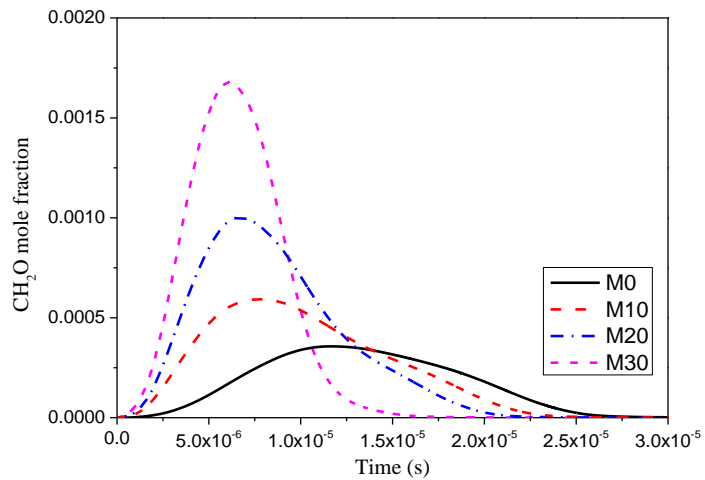
Number	C <sub>8</sub> H <sub>18</sub>	C <sub>7</sub> H <sub>16</sub>	C <sub>6</sub> H <sub>5</sub> CH <sub>3</sub>	CH <sub>3</sub> OH
M0	0.420	0.150	0.430	0
M10	0.387	0.135	0.378	0.1
M20	0.344	0.120	0.336	0.2
M30	0.301	0.105	0.294	0.3
M40	0.258	0.090	0.252	0.4



366

367

Fig.17. The heat release rate comparison for different volume fractions of methanol in TRF fuel.



368

369

Fig.18. The effect of methanol volume fraction on CH<sub>2</sub>O emissions.

370

371

372

373

374

375

376

377

378

379

380

381

382

Figure 18 shows the effect of methanol volume fraction on CH<sub>2</sub>O emissions with  $T=1400$  K,  $p=5.07$  MPa, and  $\phi=1.0$ . It can be seen from Fig. 16 that as the proportion of methanol increases, the CH<sub>2</sub>O mole fraction gradually goes up accordingly. When blending 20% methanol in TRF, the emission of formaldehyde is doubled compared to the TRF. This is a good explanation why methanol blending ratio in gasoline is generally 5%, 10% and 15%, as its purpose is to control the emission deterioration of formaldehyde.

## 5. Conclusions

(1) A new reduced chemical kinetics mechanism for the four components alternative fuel (methanol, n-heptane, isooctane and toluene) including 100 species and 290 reactions was developed based on the SA and reaction pathway analysis methods, which was verified by shock tube, flow reactor and HCCI engine. The results show great agreement with experimental data and present the dependence of ignition delays on octane value.

(2) The main intermediates of methanol oxidation were determined by sensitivity analysis method, and then the reaction kinetics analysis method was used to understand and select key consumption pathways of

383 important intermediates. A reduced methanol mechanism was constructed, consisting 24 species and 57  
384 reactions, and it was verified by shock tube and flow reactor model.

385 (3) Using the temperature sensitivity analysis, four preliminary simplified kinetic models of TRF with  
386 different components and reactions was obtained. The simplified mechanism was selected when the threshold  
387 is 0.05, including 98 components and 247 reactions. Then, using the reaction rate analysis to integrate the  
388 whole mechanism, the final vision of TRF reduced mechanism was built, including 98 components and 264  
389 reactions, and it is successfully verified via shock tube and HCCI engine model.

390 (4) The methanol simplification mechanism was added to the TRF simplification mechanism, and a  
391 four-component mixed simplification kinetic mechanism consisting of 100 components and 290 elementary  
392 reactions was constructed

393 (5) The effects of different methanol blending ratios on TRF combustion characteristics and emissions  
394 were investigated using a simplified four-component mixing mechanism. The results show that methanol  
395 inhibits the secondary oxidation process of TRF components. As the methanol volume fraction increasing,  
396 the exothermic start time is advanced, and the exothermic rate peak and total heat release increase. However,  
397 the burning duration is reduced. Therefore, exothermic peak and ignition timing can be controlled by  
398 changing the ratio of fuel components.

399 (6)The molar fraction of  $\text{CH}_2\text{O}$  increases with the increase of methanol concentration. When the  
400 concentration of methanol in TRF reaches 20%, formaldehyde emission is doubled compared with original  
401 toluene reference fuel.

## 402 **References**

- [1] Han D, Ickes A M, Bohac S V, et al. Premixed low-temperature combustion of blends of diesel and gasoline in a high speed compression ignition engine[J]. Proceedings of the Combustion Institutes, 2009, 33(2):3039-3046.
- [2] Dec, John E. "Advanced compression-ignition engines—understanding the in-cylinder processes." Proceedings of the combustion institute 32.2 (2009): 2727-2742.
- [3] Bendu, Harisankar, and S. Murugan. "Homogeneous charge compression ignition (HCCI) combustion: Mixture preparation and control strategies in diesel engines." Renewable and Sustainable Energy Reviews 38 (2014): 732-746.
- [4] Lawler, Benjamin, et al. "Thermally Stratified Compression Ignition: A new advanced low temperature combustion mode with load flexibility." Applied energy 189 (2017): 122-132.
- [5] Lu, Xingcai, Dong Han, and Zhen Huang. "Fuel design and management for the control of advanced compression-ignition combustion modes." Progress in Energy and Combustion Science 37.6 (2011): 741-783.

- [6] Yap D, Megaritis A, Wyszynski ML. "An investigation into bioethanol homogeneous charge compression ignition (HCCI) engine operation with residual gas trapping," *Energy & Fuels* 2004;18(5):1315–23.
- [7] Noguchi M, Tanaka Y, Tanaka T, Takeuchi Y. "A study on gasoline engine combustion by observation of intermediate reactive products during combustion," SAE Technical Paper Series No. 790840; 1979
- [8] M. Bahattin Çelik, Bülent Özdalyan, Faruk Alkan. The use of pure methanol as fuel at high compression ratio in a single cylinder gasoline engine[J]. *Fuel*, 2011, 90(4):1591-1598.
- [9] Turner J W G, Pearson R J, Dekker E, et al. Extending the role of alcohols as transport fuels using iso-stoichiometric ternary blends of gasoline, ethanol and methanol[J]. *Applied Energy*, 2013, 102(2):72-86.
- [10] Mehl M., Pitz W. J., Westbrook C. K., et al. Kinetic modeling of gasoline surrogate components and mixtures under engine conditions [J]. *Proceedings of the Combustion Institutes*, 2011, 33(1): 193-200.
- [11] American Society for Testing and Materials, Annual Book of ASTM Standards. Test methods for rating motor, diesel and aviation fuels (05.04), 1993.
- [12] Mittal G., Sung C. J. Autoignition of toluene and benzene at elevated pressures in a rapid compression machine [J]. *Combustion and Flame*, 2007, 150(4): 355-368.
- [13] Andrae J C G, Brinck T, Kalghatgi G T. HCCI experiments with toluene reference fuels modeled by a semidetailed chemical kinetic model[J]. *Combustion & Flame*, 2008, 155(4):696-712.
- [14] Bowman C T. A shock-tube investigation of the high-temperature oxidation of methanol[J]. *Combustion and Flame*, 1975, 25: 343-354.
- [15] Held T J, Dryer F L. A comprehensive mechanism for methanol oxidation [J]. *International Journal of Chemical Kinetics*, 1998, 30 (11): 805-830.
- [16] Aronowitz D, Santoro R J, Dryer F L, et al. Kinetics of the oxidation of methanol: Experimental results semi-global modeling and mechanistic concepts[C]//Symposium (International) on Combustion. Elsevier, 1979, 17(1): 633-644.
- [17] Westbrook C K, Dryer F L. Comprehensive mechanism for methanol oxidation[J]. *Combustion Science and Technology*, 1979, 20(3-4): 125-140.
- [18] Thomas S. Norton, Frederick L. Dryer. Some New Observations on Methanol Oxidation Chemistry[J]. *Combustion Science and Technology*, 1989, 63(1-3):107-129.
- [19] Tsang W. Chemical Kinetic Data Base for Combustion Chemistry. Part 2. Methanol[J]. *Journal of Physical and Chemical Reference Data*, 1987, 16(3):471-508.
- [20] Li J, Zhao Z, Kazakov A, et al. A comprehensive kinetic mechanism for CO, CH<sub>2</sub>O, and CH<sub>3</sub>OH combustion[J]. *International Journal of Chemical Kinetics*, 2007, 39(3): 109-136.
- [21] Smith G P, Golden D M, Frenklach M, et al. GRI-Mech 3.0[J]. URL: [http://www. me. berkeley. edu/gri\\_mech](http://www.me.berkeley.edu/gri_mech), 1999, 51: 55.
- [22] Zhang F, Shuai S, Wang Z, et al. A detailed oxidation mechanism for the prediction of formaldehyde emission from methanol-gasoline SI engines[J]. *Proceedings of the Combustion Institute*, 2011, 33(2):3151-3158.

- [23] Burke U, Metcalfe W K, Burke S M, et al. A detailed chemical kinetic modeling, ignition delay time and jet-stirred reactor study of methanol oxidation[J]. *Combustion and Flame*, 2016, 165(5):125-136.
- [24] Qingfeng Zhang, Zhaolei Zheng, Zuwei He. Reduced chemical kinetic model of toluene reference fuels for HCCI combustion[J]. *Acta Phys.-Chim. Sinica*, 2009, 27(3): 530-538.
- [25] Heghes C., Morgan N., Riedel U., et al. Development and validation of a gasoline surrogate fuel kinetic mechanism [C]. SAE Paper 2009-01-0934, 2009.
- [26] Mehl M., Chen J. Y., Pitz W. J., et al. An approach for formulating surrogates for gasoline with application toward a reduced surrogate mechanism for CFD engine modeling [J]. *Energy & Fuels*, 2011, 25(11): 5215-5223.
- [27] Andrae J. C. G., Bjornbom P., Cracknell R. F., et al. Autoignition of toluene reference fuels at high pressures modeled with detailed chemical kinetics [J]. *Combustion and Flame*, 2007, 149(1-2): 2-24.
- [28] Sakai Y., Miyoshi A., Koshi M., et al. A kinetic modeling study on the oxidation of primary reference fuel-toluene mixtures including cross reactions between aromatics and aliphatics [J]. *Proceedings of the Combustion Institute*, 2009, 32(1): 411-418.
- [29] Ra Y., Reitz R. D. A combustion model for IC engine combustion simulations with multi-component fuels [J]. *Combustion and Flame*, 2011, 158(1): 69-90.
- [30] S. H. Lam. Reduced Chemistry Modeling and Sensitivity Analysis [J]. *Lecture Notes for Aerothermochemistry for Hypersonic Technology (April 24–28, 1995)*, pp. 1994-1995
- [31] R. J. Kee, F. M. Rupley, J. A. Miller, M. E. Coltrin, J. F. Gracar, E. Meeks, H. K. Moffat, A. E. Lutz, G. Dixon-Lewis, M. D. Smooke, J. Warnatz, G. H. Evans, R. S. Larson, R. E. Mitchell, L. R. Petzold, W. C. Reynolds, M. Caracotsios, W. E. Stewart, P. Glarborg, C. Wang, C. L. McLellan, O. Adigun, W. G. Houf, C. P. Chou, S. F. Miller, P. Ho, P. D. Young, D. J. Young, D. W. Hodgson, M. V. Petrova, and K. V. Pudukkham, CHEMKIN Release 4.1, Reaction Design, San Diego, CA (2006).
- [32] T.S. Norton, F.L. Dryer, et al. Some new observations on methanol oxidation chemistry[J]. *Combust. Sci. Technol.* 63 (1989) 107.
- [33] K. Fieweger, R. Blumenthal, G. Adomeit, et al. Self-ignition of S.I. engine model fuels: A shock tube investigation at high pressure[J]. *Combust. Flame* 109 (1997) 599–619.
- [34] D.F. Davidson, B.M. Gauthier, R.K. Hanson, et al. Shock tube ignition measurements of iso-octane/air and toluene/air at high pressures[J]. *Proc. Combust. Inst.* 30 (2005) 1175–1182.
- [35] B.M. Gauthier, D.F. Davidson, R.K. Hanson, et al. Shock tube determination of ignition delay times in full-blend and surrogate fuel mixtures[J]. *Combust. Flame* 139 (2004) 300–311.
- [36] J C G Andrae, R A Head. HCCI experiments with gasoline surrogate fuels modeled by a semidetailed chemical kinetic model[J]. *Combustion and Flame*, 2009, 156(4): 842-851.